Zhang *et al. Horticulture Advances* (2026) 4:14
https://doi.org/10.1007/s44281-026-00103-z

Horticulture Advances

RESEARCH ARTICLE Open Access

Chromosome-level genome assembly reveals the genetic mechanisms underlying elite waterlogging tolerance in *Actinidia rufa*

Qiong Zhang[1,2*], Linhui Wu[1,2], Hao Zheng[1], Yule Wang[1], Zupeng Wang[1], Shaokui Yi[3], Yifei Liu[4*] and Caihong Zhong[1*]

Abstract

Actinidia rufa is a valuable species for hybridization and introgressive breeding of new kiwifruit cultivars due to its exceptional tolerance to waterlogging. In this study, a chromosome-level genome of *A. rufa* was assembled using Illumina short-read and PacBio Continuous Long Read (CLR) sequencing technologies. The assembled genome spans 613.66 Mb with an N50 of 3.06 Mb, and 94 scaffolds were anchored to 29 pseudochromosomes. A total of 42,484 protein-coding genes and 267.26 Mb of repetitive sequences, accounting for 49.08% of the genome, were identified. Phylogenetic analysis demonstrated a close evolutionary relationship between *A. rufa* and *A. chinensis*, with their most recent common ancestor being estimated to diverge around 7 million years ago. Demographic analysis indicated a historical population expansion in *A. rufa*, whose current suitable habitats are primarily found in the Japanese archipelago and Taiwan, China. Comparative genomic analysis revealed large-scale structural variations, including a chromosomal region on Chr19 in *A. rufa* that corresponds to two distinct segments on Chr2 and Chr9 in *A. chinensis*. Additionally, *A. rufa* cv. 'MTS7001' exhibited superior waterlogging tolerance compared to *A. chinensis* cv. 'Donghong'. Gene expression analysis showed that, in response to early waterlogging stress, *A. rufa* exhibited upregulation of genes associated with energy metabolism and signaling of hormones, including those related to auxin, abscisic acid, and brassinosteroids, compared to *A. chinensis*. This study provides genomic insights into the genetic basis of exceptional waterlogging tolerance in *A. rufa*, contributing to molecular breeding efforts in kiwifruits in the future.

Keywords Kiwifruit, *Actinidia*, Gene regulation, Waterlogging stress, RNA-seq

*Correspondence:
Qiong Zhang
qiongzhang@wbgcas.cn
Yifei Liu
liuyifei@hbtcm.edu.cn
Caihong Zhong
zhongch@wbgcas.cn
[1] State Key Laboratory of Plant Diversity and Specialty Crops, Wuhan Botanical Garden, Chinese Academy of Sciences, Wuhan 430074, People's Republic of China
[2] College of Life Sciences, University of Chinese Academy of Sciences, Beijing 101408, People's Republic of China
[3] College of Life Sciences, Huzhou University, Huzhou 313000, People's Republic of China
[4] College of Pharmacy, Hubei University of Chinese Medicine, Wuhan 430065, People's Republic of China

Introduction

Kiwifruit (*Actinidia* Lindl.) is renowned as the "king of fruits" due to its exceptional nutritional value and proven health benefits (Wu et al. 2025a, b, c). Endemic to southwestern China (Zhang et al. 2023), the genus has diversified globally, now encompassing approximately 54 species (x = 29) (Wu et al. 2025a, b, c). However, commercial cultivation is dominated by just two taxa—*Actinidia chinensis* var. chinensis and var. deliciosa—which together account for the majority of the over 100 recognized cultivars (Huang and Liu 2014; Wang et al. 2021). This limited genetic diversity contrasts with the extensive natural variation within *Actinidia*, such as the high vitamin C content in *A. latifolia* and the combination of

sweetness and unique color in red-fleshed *A. chinensis* accessions (Wang et al. 2025; Yuan et al. 2022). Kiwifruit is widely recognized as a superfood, rich in antioxidants and anti-inflammatory compounds (Suleria et al. 2020), and its underutilized byproducts, including peels, seeds, pulp, and pruning residues, offer valuable sources of phenolic compounds and antioxidant activity for industrial use (Gubitosa et al. 2022; Sanz et al. 2021).

Typically, *Actinidia* species are sensitive to waterlogging stress, making grafting onto waterlogging-tolerant rootstocks a practical approach to enhance plant adaptation. Root anoxia, induced by waterlogging, poses a significant challenge to plant survival and growth. Native to the humid coastal regions of Japan, *Actinidia rufa* naturally thrives in low temperatures and waterlogged soils—traits rarely found among commercial kiwifruit species. Through prolonged natural selection, *A. rufa* has developed robust genetic resources for stress resistance, particularly notable for its exceptional waterlogging tolerance. As a close relative of *A. chinensis* var. chinensis, *A. rufa* represents a valuable genetic resource for cultivar improvement (Liu et al. 2017). Recently, *A. rufa* has gained commercial attention, with its hybrid with *A. chinensis*, 'Zhongkelvmi No. 9', not only inheriting waterlogging resistance but also featuring high sugar content and a distinctive aroma (Zhong et al. 2024). Previous research (Miller et al. 1997) demonstrated that *A. rufa* exhibited the highest adaptability to root anoxia among five *Actinidia* species, including *A. deliciosa*, *A. chinensis*, *A. eriantha*, *A. rufa*, and *A. hemsleyana*. In breeding practices, vines grafted onto *A. rufa* rootstocks showed enhanced photosynthetic efficiency and root respiratory activity compared to those grafted onto *A. chinensis* and *A. arguta* (Suezawa et al. 2018). Overall, *A. rufa* is not only commercially promising but also offers significant environmental resilience and genetic compatibility with major kiwifruit species, positioning it as a key resource for rootstock improvement and waterlogging tolerance breeding. Identifying and harnessing waterlogging-tolerant genes from wild resources like *A. rufa* are essential for developing resistant cultivars and promoting sustainable kiwifruit production. However, the genetic mechanisms underlying *A. rufa*'s remarkable waterlogging adaptability remain underexplored.

Since the release of the first genome of *A. chinensis* (2n = 58) in 2013 (Huang et al. 2013), high-quality genomes have become essential for elucidating the genetic basis of economically important traits in kiwifruit. Over the past decade, chromosome-scale assemblies of various *Actinidia* species have been published, including three cultivars of *A. chinensis* (Wu et al. 2019; Xia et al. 2023), two cultivars of *A. eriantha* (Tang et al. 2019; Yao et al. 2022), as well as *A. arguta*, *A. polygama*, *A. rufa*, *A. zhejiangensis*, and *A. hemsleyana* (Akagi et al. 2023; Yu et al. 2023). Notably, gap-free genomes of *A. chinensis* cv. 'Hongyang' (Yue et al. 2023), cv. 'Donghong', *A. latifolia* (Han et al. 2022), and *A. eriantha* (Wang et al. 2023) have been reported. These pangenomic resources serve as critical foundations for molecular breeding and functional studies (Li et al. 2025; Xu et al. 2026). Among the newly sequenced species, *A. rufa* is distinguished as a valuable reservoir of resilience alleles for cultivar improvement, due to its high tolerance to waterlogging, thermal stress, and robust field resistance to *Pseudomonas syringae* pv. *Actinidiae*, the most devastating bacterial pathogen of kiwifruit (Kisaki et al. 2018).

To explore the genetic mechanisms underlying root anoxia tolerance induced by waterlogging stress, a high-quality chromosome-level genome assembly of *A. rufa* was constructed using PacBio Continuous Long Read (CLR) sequencing and BioNano methods. A comparative genomic analysis of *Actinidia* species was conducted to identify genes associated with waterlogging stress adaptations in kiwifruit, which will support the development of new breeding programs aimed at improving kiwifruit resilience.

Materials and methods

Plant materials and sample collection

Young leaves were collected from the elite *A. rufa* line ('MT570001') at the Wuhan Botanical Garden, China. For DNA sequencing, genomic DNA was extracted from the young leaves. DNA quality and quantity were assessed using a NanoDrop 2000 (Thermo Fisher Scientific, Waltham, MA, USA) and agarose gel electrophoresis, respectively. For RNA-seq, root tissues were collected for RNA extraction and library preparation.

Genome survey

A 300-bp insert library was constructed using the Illumina TruSeq DNA Sample Prep Kit, following the manufacturer's protocol. Short-read sequencing was performed on an Illumina HiSeq X Ten platform in paired-end 150 bp (PE150) mode. Raw data were filtered using the fastp program (Chen et al. 2018; Chen 2023). *K*-mer analysis ($K = 17$) was performed to estimate the genome size and heterozygosity of the *A. rufa* genome, based on the clean RNA-seq reads, which were obtained after quality control, adapter removal, and elimination of low-quality sequences. Genome size was estimated using the formula: *K*-mer number/*K*-mer depth.

PacBio sequencing and genome assembly

A 20-kb PacBio library was constructed for long-read sequencing. DNA was fragmented and subjected to end repair. The library fragment size was assessed using

an Agilent 2100 Bioanalyzer (2100, Agilent Technologies, America). Sequencing was performed on a PacBio Sequel platform (Pacific Biosciences, America). FALCON (Chin et al. 2016) was used to assemble the long reads with the following parameters: length_cutoff_pr = 5000, max_diff = 120, max_cov = 130. Primary contigs were generated using FALCON-Unzip and then polished with Quiver v2.3.3.

Extending scaffolds with 10× Genomics and a genetic map

Sample preparation for the GemCode system of 10× Genomics was carried out using 1 ng of DNA for the gel beads-in-emulsion (GEM) reaction. DNA was sheared into 500-bp fragments for library construction, which were sequenced on an Illumina HiSeq system. Burrows-Wheeler Alignment tool (BWA) (Li and Durbin 2009) was employed to map the reads from 10 × Genomics to the contigs, and fragScaff (Adey et al. 2014) was used for scaffolding. The flanking sequences (200 bp) of the SNP sites from the genetic map (Zhang et al. 2015a, b) were extracted and mapped to the assembly. The flanking sequences aligned uniquely to the contigs, which were then ordered and integrated into 29 pseudochromosomes using Chromonomer v1.11. The assembled sequences were polished using POLCA (Zimin and Salzberg 2020), and short reads were generated for the genome survey. Assembly completeness was assessed using the Bench Marking Universal Single-copy Orthologs (BUSCO) with the embryophyta_odb10 database (Simao et al. 2015).

Repetitive element and protein-coding gene annotation

Homology-based and de novo prediction methods were employed to identify repetitive elements in the genome. Transposable elements (TEs) were detected using RepeatMasker (Tarailo-Graovac and Chen 2009) with Repbase (Bao et al. 2015), and RepeatProteinMask was utilized to search the TE protein database. Additionally, a de novo repeat database was constructed using RepeatModeler (Flynn et al. 2020). Long terminal repeat (LTR) retrotransposons and tandem repeats were detected with LTR_FINDER v1.0.7 (Xu and Wang 2007) and Tandem Repeat Finder (Benson 1999), respectively. Finally, the libraries generated from both methods were integrated using RepeatMasker.

Protein-coding genes (PCGs) were predicted through ab initio, homology-based, and transcript-based methods. Ab initio predictions were made using Augustus (Nachtweide and Stanke 2019) and GeneScan V1.0. Homology-based predictions were carried out with Exonerate v2.2.0 (Slater and Birney 2005) to align the protein sequences of kiwifruit species. RNA-Seq data were assembled into transcripts using Trinity software (Haas et al. 2013), and gene models were predicted from 86,014 transcripts using PASA v2.0.1. The non-redundant gene set was obtained by integrating gene models with EVidenceModeler (EVM) (Haas et al. 2007).

Genome evolution and comparative genomic analyses

To explore the evolutionary history of *A. rufa*, OrthoFinder2 (Emms and Kelly 2019) was used to identify gene families and orthologous genes. Single-copy gene families were detected through all-against-all protein searches from six kiwifruit cultivars: *A. rufa*, *A. latifolia*, *A. chinensis* cv. 'Hongyang', *A. chinensis* cv. 'Donghong', *A. polygama*, *A. eriantha* cv. 'White', and nine closely related species, including *Rhododendron delavayi*, *Camellia sinensis*, *Solanum lycopersicum*, *Camellia arabica*, *Camellia nankingense*, *Vitis vinifera*, *Malus domestica*, *Pyrus communis*, and *Arabidopsis thaliana*. Phylogenetic tree construction and divergence time estimation were based on 101 single-copy orthologous genes (SOGs). A phylogenetic tree was built with FastTree using the divergence time between apple and pear as a calibration scale (Price et al. 2009). Gene family expansion and contraction were identified using CAFE v4.2.1 (De Bie et al. 2006). Species divergence times were inferred using MCMCTree in the PAML package (Yang 2007), and species-specific genes were identified from OrthoFinder2 output.

Syntenic blocks with more than five collinear genes were identified among *A. rufa*, *A. polygama*, and *A. chinensis* cv. 'Hongyang' using the JCVI package (Tang et al. 2024) with default parameters. Orthologous genes were detected through reciprocal BLAST hits, and protein alignments were conducted with ParaAT (Zhang et al. 2012) using default settings. *Ka*/*Ks* ratios were calculated on a branch-wise basis using CodeML with a branch model (Gao et al. 2019).

Structural variation (SV) identification

To detect deletions and insertions among the genomes, assemblies were mapped to the reference genome using the nucmer program, and alignment blocks were filtered using a delta filter in 1-to-1 alignment mode. SNPs and insertions/deletions (InDels) were identified from 1-to-1 blocks using the show-snps function in the MUMmer4 toolkit. Insertion and deletion events were ultimately detected using the BEDtools v2.31 subtract function, with deletions in both alignments being converted into presence/absence variations (PAVs).

Population demographic history and species distribution modeling (SDM)

Genome resequencing was performed on individuals from kiwifruit cultivars using an Illumina HiSeq platform. Following quality control, the clean reads were

mapped to the reference genome using BWA. SNP calling was executed using the HaplotypeCaller function in Genome Analysis Toolkit (GATK) (McKenna et al. 2010). To infer population size trajectories and divergence times of the kiwifruit cultivars, SMC++ (Terhorst et al. 2017) was applied. The SMC++ pairwise dataset was formatted using vcf2smc, with the mutation rate (μ) set to 2×10^{-8} per generation and the generation time set at 6 years.

Species distributions over time were modeled using Maxent v3.4.1 (https://github.com/mrmaxent/Maxent) (Vollering et al. 2019). Presence data for *A. rufa* were collected from specimen records in variable herbariums and from the Global Biodiversity Information Facility (http://www.gbif.org/). Nineteen bioclimatic variables for four distinct time periods were downloaded from the WorldClim database (https://worldclim.org/). Pearson's correlation analyses were performed to filter highly correlated variables. The model was optimized using an Akaike information criterion (AIC)-based method and further validated with random cross-validation. The four time periods included in the modeling were the Last Glacial Maximum (LGM) (~0.022 Mya), the Mid-Holocene (MH) (~0.006 Mya), the current day (historical data from 1970 to 2000), and the projected future period (2061–2080).

Physiological and biochemical measurements

Key physiological and biochemical parameters were assessed using standard methods. Leaf relative water content (RWC) was determined gravimetrically by measuring both fresh and oven-dried weights. Hydrogen peroxide (H_2O_2) content was quantified spectrophotometrically at 415 nm following acetone extraction and a series of reagent reactions, with calculations based on a standard curve. Malondialdehyde (MDA) concentration, indicating lipid peroxidation, was measured using the thiobarbituric acid (TBA) method, with absorbance readings at 450, 532, and 600 nm. Superoxide dismutase (SOD) activity was assayed *via* the nitroblue tetrazolium (NBT) photochemical reduction method, with activity expressed in units per milligram fresh weight. The net photosynthetic rate (Pn) and stomatal conductance (Gs) were recorded using a portable photosynthesis system (LI-6400, Heinz Walz GmbH, Effeltrich, Germany) under stable ambient conditions.

Transcriptome analysis

A. rufa cv. 'MTS7001' (SL) and *A. chinensis* cv. 'Donghong' (DH), representing waterlogging-tolerant and waterlogging-sensitive kiwifruit species, respectively, were selected for this study. Root tissues from SL and DH plants subjected to waterlogging for 0 h (R0), 12 h (R12), 24 h (R24), 48 h (R48), and 72 h (R72) were collected for RNA extraction and Illumina HiSeq sequencing. RNA was extracted using the RNAiso Kit (TaKaRa, China). A total of 30 RNA-Seq libraries were constructed and sequenced on an Illumina HiSeq system.

Analysis of gene expression patterns under waterlogging stress

Clean reads from each sample were mapped to the reference genome using TopHat2 (Kim et al. 2013). Gene expression levels were normalized to FPKM values. Differentially expressed genes (DEGs) were identified using the DESeq2 package in R (Love et al. 2014). Gene Ontology (GO) and Kyoto Encyclopedia of Genes and Genomes (KEGG) pathway enrichment analyses of the DEGs from pairwise comparisons were performed. Genes with low expression (FPKM < 10) were excluded, and the remaining DEGs were selected for coexpression network analysis using weighted gene coexpression network analysis (WGCNA) (Langfelder and Horvath 2008). Coexpression modules were detected using the automatic network construction function, with a soft threshold power of 16, as determined by the pickSoftThreshold function in the WGCNA package. Candidate genes were selected from WGCNA modules that exhibited low expression in DH and high expression in *A. rufa*.

Statistical analysis

The experimental data were preliminarily collated and analyzed by Microsoft Excel 2021, and the mean and standard deviation of each quality index were calculated by SPSS 20.0 software. All the data are expressed as the mean ± standard deviation. Statistical significance was determined using Student's *t*-test, and differences were considered significant at $P<0.05$. Analysis of significant differences was performed with GraphPad Prism 8 and SPSS 20.0.

Results

Genome assembly and annotation

An individual of *A. rufa* (Fig. 1a) was selected for Illumina and PacBio sequencing. Initially, 61.61 Gb of Illumina paired-end reads were generated and analyzed with a 17-mer frequency distribution, predicting a genome size of ~635.84 Mb, a heterozygosity of 0.65%, and a repeat content of 44.07% (Fig. S1). A total of 60.45 Gb of PacBio CLR reads (~95.08-fold genome coverage) were assembled into 467 contigs. The genome assembly was 613.66 Mb in length, with the longest contig spanning 16.18 Mb and a contig N50 of 3.06 Mb. A total of 111.11 Gb of 10× Genomics linked reads were used for scaffolding, resulting in 222 scaffolds with a scaffold N50 of 5.05 Mb. Mapping the Illumina data back to the final assembly yielded a mapping rate of 98.03%, and

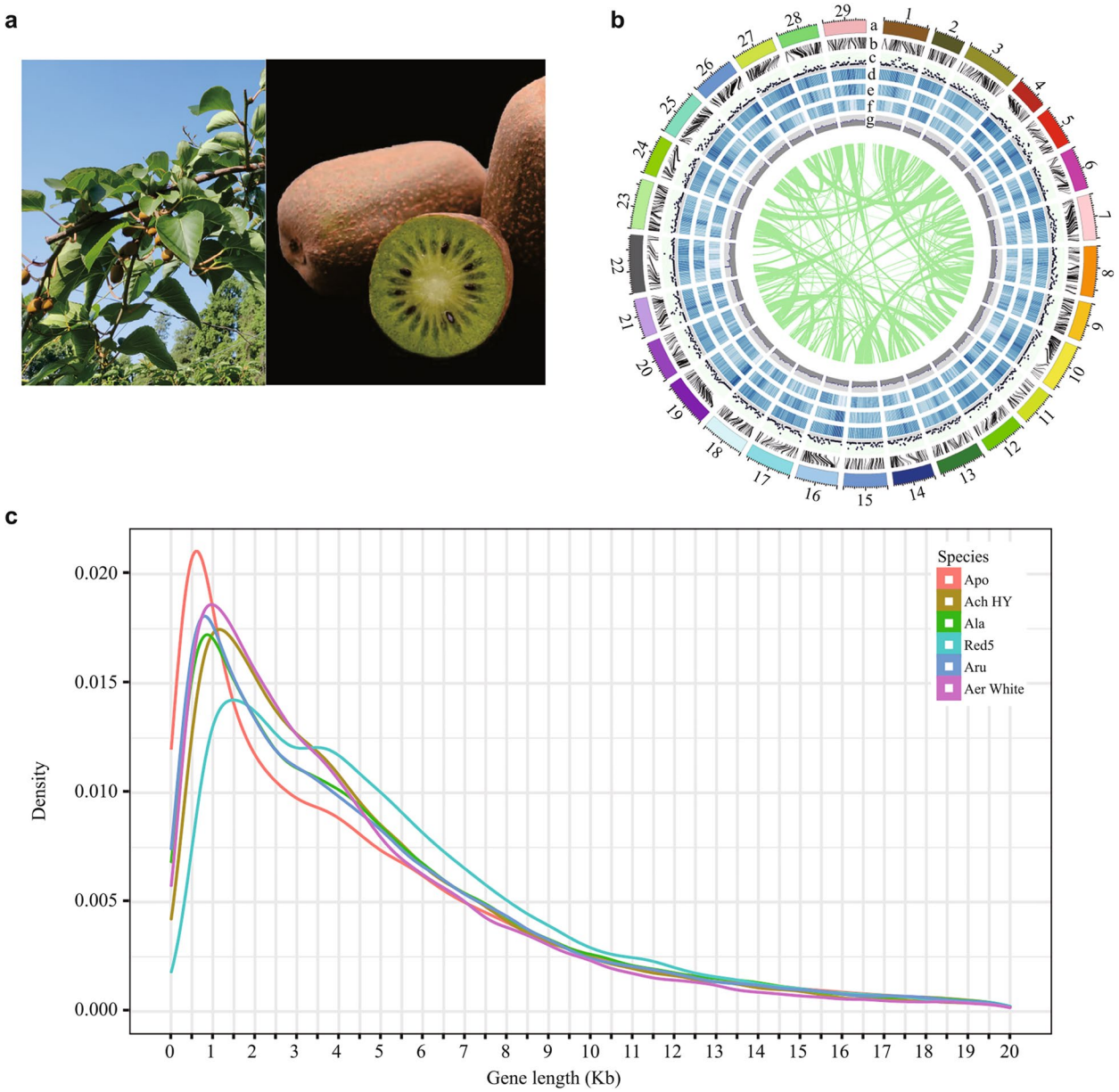

Fig. 1 Genomic features of *Actinidia rufa*. **a** A fruit of *A. rufa*. **b** The genome landscape of *A. rufa*. Track a, chromosome coordinates; Track b, genetic linkage map and genome collinearity; Track c, gene count; Track d, repeat element density; Track e, long terminal repeat (LTR) density; Track f, tandem repeat density; Track g, GC content distribution. All were calculated in a 500-kb window. The inner links represent collinear blocks (minimum size 100 kb). **c** Length distribution of the predicted genes in kiwifruit genomes. Apo, *Actinidia polygama*; Ach HY, *A. chinensis* cv. 'Hongyang'; Ala, *A. latifolia*; Red5, *A. chinensis* cv. 'Red5'; Aru, *A. rufa*; Aer White, *A. eriantha* cv. 'White'

Core Eukaryotic Genes Mapping Approach (CEGMA) analysis recovered 96.77% of the core eukaryotic genes, collectively confirming the high quality of the reference genome.

The genome assembly was further anchored into pseudochromosomes using a genetic linkage map composed of 2426 SNPs across 29 linkage groups (LGs), with a total length of 2,651 cM. In total, 93 scaffolds (615.28 Mb; scaffold N50 = 19.84 Mb) were ordered, with the 29 longest scaffolds corresponding to the 29 chromosomes, spanning 578.54 Mb, or 94.03% of the total assembly (Fig. 1b). Additionally, BUSCO analysis revealed that the genome assembly had 96.4% completeness, based on the Embryophyta_odb10 dataset.

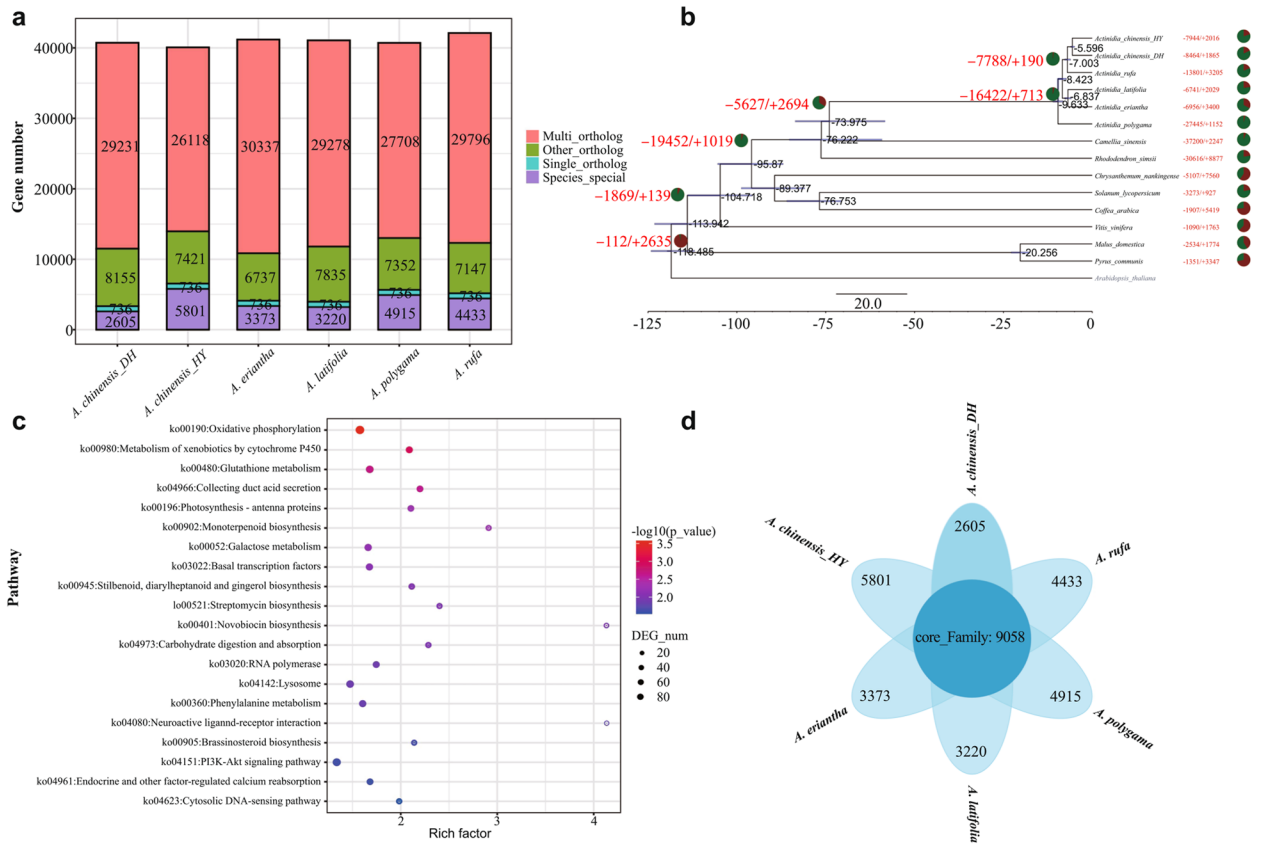

Fig. 2 Evolution and comparative genomic analysis of *Actinidia rufa*. **a** Number of gene families shared between *A. rufa* and the other species. *A. chinensis* DH, *Actinidia chinensis* cv. 'Donghong'; *A. chinensis* HY, *Actinidia chinensis* cv. 'Hongyang'. **b** Phylogenetic analysis of *A. rufa* and other asterid plants. **c** Kyoto Encyclopedia of Genes and Genomes (KEGG) enrichment of the expanded gene families in *A. rufa*. DEGs, differentially expressed genes. **d** Venn diagram of the species-specific gene families

Repetitive DNA sequences accounted for 267.26 Mb (43.44%) of the genome, predominantly composed of 168.54 Mb of LTR retrotransposons (27.39%) and 59.82 Mb of DNA transposons (9.72%) (Table S1). A total of 42,484 PCGs were predicted, with an average gene length of 5,518 bp and a mean CDS length of 1,059 bp (Fig. 1c). Of these, 94% of the PCGs were functionally annotated using public databases, while 2,568 gene models remained unannotated.

Identification of gene families and genome evolution

A total of 101 SOGs were identified from 15 species and used to construct a phylogenetic tree. Additionally, PCGs from six kiwifruit taxa—*A. rufa*, *A. latifolia*, *A. chinensis* cv. 'Hongyang' (v3), *A. chinensis* cv. 'Donghong', *A. polygama*, and *A. eriantha* cv. 'White'—were clustered, identifying 736 shared SOG families across all six taxa (Fig. 2a). Phylogenetic analysis revealed that *A. rufa* is most closely related to the two *A. chinensis* cultivars (Fig. 2b), with the most recent common ancestor (MRCA) of *A. rufa* and the *A. chinensis* cultivars diverging approximately 7 million years ago (Mya). Furthermore, *Actinidia* species were more closely related to *Rhododendron delavayi* and *Camellia* sinensis.

A total of 2,785 gene families in *A. rufa* underwent expansion, while 13,214 gene families contracted (Fig. 2b). Expanded gene families were significantly enriched in GO terms such as "SOD activity", "oxidative phosphorylation", and "superoxide metabolic process", along with several KEGG pathways, including "monoterpenoid biosynthesis", "oxidative phosphorylation", and "photosynthesis-antenna proteins" (Fig. 2c). Genes associated with hypoxic tolerance, including *SEEDSTICK* (*STK*), *beta-N-acetylhexosaminidase-1* (*Hex-1*), *Hex-3*, and *eukaryotic Translation Initiation Factor 5A* (*eIF5A*), were detected in enriched pathways, highlighting their role in waterlogging tolerance (Zhou et al. 2023; R Kumar et al. 2017; I Alam et al. 2010). Conversely, contracted gene families were enriched in GO terms such as "oxidation–reduction process", "oxidoreductase activity", "heme binding", "tetrapyrrole binding", and "mitochondrial envelope". Of the 42,112 PCGs, 34,185 were assigned to

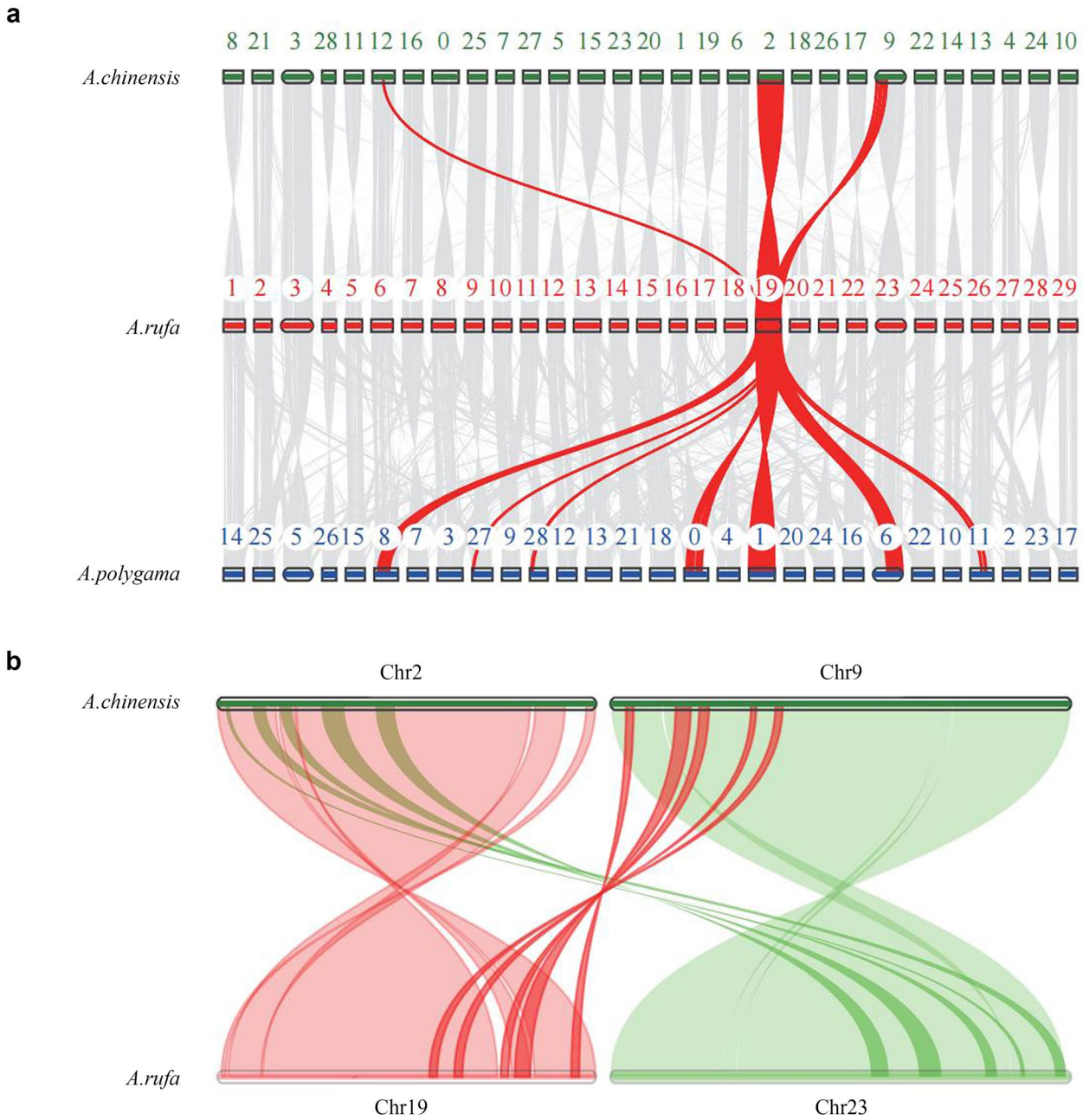

Fig. 3 Syntenic analysis among *Actinidia* genomes. **a** Collinearity pattern between the *A. rufa*, *A. chinensis*, and *A. polygama* genomes. Gray wedges connect matching gene pairs, with one highlighted in red. **b** Synteny between Chr19 of *A. rufa* and Chr2 and Chr9 of *A. chinensis*

13,205 gene families, with an average of 2.59 genes per family, while 4,433 genes were *A. rufa*-specific (Fig. 2d). Pfam enrichment analysis revealed that the *A. rufa*-specific genes were significantly enriched in the "PPR repeat family", "pentatricopeptide repeat domain", and "leucine-rich repeat" families.

Comparative genomics of *Actinidia* species

The conserved synteny between *A. rufa*, *A. polygama*, and *A. chinensis* cv. 'Hongyang' was examined. Most chromosomes showed a high level of conserved synteny across the three species (Fig. 3). Notably, Chr19 of *A. rufa* exhibited orthologous regions with multiple chromosomes from both *A. chinensis* cv. 'Hongyang'

and *A. polygama* (Fig. 3a), indicating chromosome fission or fusion events occurred after their speciation. Inversions were also observed between *A. rufa* and *A. chinensis* cv. 'Hongyang', including inversions on Chr19 of *A. rufa* and Chr2 of *A. chinensis* cv. 'Hongyang'. Specifically, a region on Chr19 of *A. rufa* was found to have two copies on Chr2 and Chr9 of the *A. chinensis* genome (Fig. 3b). A total of 412 genes (Table S2) were located within this region, and KEGG enrichment analysis revealed significant pathways such as cAMP signaling, steroid biosynthesis, proteasome function, and Epstein–Barr virus infection. Notably, two copies of *histone acetyltransferase* (*HATs*) and *RING-box protein-like* (*RBXs*) were detected in the *A. chinensis* genome. Among these 412 genes, key factors such as APETALA 2 (AP2)-like factors, *BRCA1*/*BRCA2*, and *WRKY* transcription factors—known to be involved in waterlogging and drought stress resistance—were identified.

The chromosomes of *A. rufa* were aligned to the genomes of *A. chinensis* (cv. 'Hongyang' and 'Red5'). Through the alignment of 1-to-1 syntenic blocks between *A. rufa* and *A. chinensis* genomes, a total of 16,198,692 SNPs and 4,276,640 InDels were identified. Further comparison between the *A. rufa* and *A. chinensis* genomes revealed 4,588 *A. rufa*-specific genomic segments (~ 73.59 Mb) longer than 10 kb, representing PAVs. These PAVs were unevenly distributed across chromosomes, with clustering observed on Chr22, Chr28, and Chr29. The PAV genes were significantly enriched in pathways such as "carotenoid biosynthesis" and "cutin, suberin, and wax biosynthesis".

Demographic history and species distribution dynamics

Demographic analysis based on SMC++ clearly indicated a significant population expansion of *A. rufa* around 17.8 Mya. In contrast, populations of *A. eriantha*, *A. latifolia*, and *A. polygama* showed a decline starting around 31.6 Mya. These analyses further suggested that after the population decline, the kiwifruit species experienced population stability (Fig. S2). Species distribution modeling revealed that Model H1 produced the lowest AIC value. The suitable distribution areas for *A. rufa* contracted from the LGM to the MH, with a notable increase in the central regions of China (Fig. 4a, b). However, from the MH to the present, suitable areas in central and southern China diminished (Fig. 4c). The Japanese and Taiwanese islands consistently exhibited the highest habitat suitability across all climate scenarios. Projections for the future suggest that the suitable regions for *A. rufa* will retreat significantly to the East Asian islands (Fig. 4d).

Physiological differences between *A. rufa* and *A. chinensis* under waterlogging stress

To assess the physiological response to waterlogging, leaves from *A. rufa* cv. 'MTS7001' and *A. chinensis* cv. 'Donghong' were collected at 0, 12, 24, 48, 72 h and 7 d after submergence treatment (Fig. 5a). As waterlogging stress progressed, *A. rufa* cv. 'MTS7001' demonstrated superior tolerance compared to the control cultivar *A. chinensis* cv. 'Donghong'. In addition, 'MTS7001' exhibited a more gradual decline and maintained a higher RWC, particularly after 72 h of treatment (Fig. 5b). As for oxidative stress, the H_2O_2 levels in 'MTS7001' were significantly lower than those in 'Donghong' from 12 h to 7 d, indicating enhanced reactive oxygen species (ROS) scavenging capacity in 'MTS7001'. In addition, SOD activity increased in both cultivars under waterlogging stress (Fig. 5d). 'MTS7001' exhibited lower levels of MDA relative to 'Donghong', implying the former suffered from less serious membrane lipid peroxidation under waterlogging stress (Fig. 5e).

Gene expression patterns of *A. rufa* with waterlogging tolerance

The clean reads from 30 samples were mapped to the genomes, with mapping ratios ranging from 85.61% to 91.30%. A total of 29,970 DEGs were detected by pairwise comparisons across the libraries (Fig. 6a). Notably, the majority of DEGs (59.53%) were identified between R0 and R12. After 12 h of waterlogging treatment, the number of DEGs in *A. rufa* significantly decreased. KEGG enrichment analysis revealed that these DEGs were primarily enriched in the pathways "plant hormone signal transduction", "flavonoid biosynthesis", and "starch and sucrose metabolism", indicating that a number of genes mediated the stress response at the early stages of waterlogging treatment. Additionally, *K*a/*K*s ratios were calculated using CodeML with a branch model to identify positively selected genes (PSGs) among the six kiwifruit cultivars. In total, 323 PSGs were identified in *A. rufa* (Fig. 6e), which were significantly enriched in the "steroid hormone biosynthesis", "monobactam biosynthesis", "plant–pathogen interaction", and "lysine biosynthesis" pathways (Fig. 6f). Among these PSGs, 247 were expressed according to the transcriptome data, with 104 upregulated in *A. rufa* compared to the 'Donghong' cultivar (Figs. S3, S4). These upregulated PSGs were enriched in "monobactam biosynthesis", "RNA degradation", "lysine biosynthesis", and "cytosolic DNA-sensing pathway", suggesting their potential role in *A. rufa*'s adaptive response to waterlogging. These findings indicate that PSGs may contribute to the species' unique environmental adaptation.

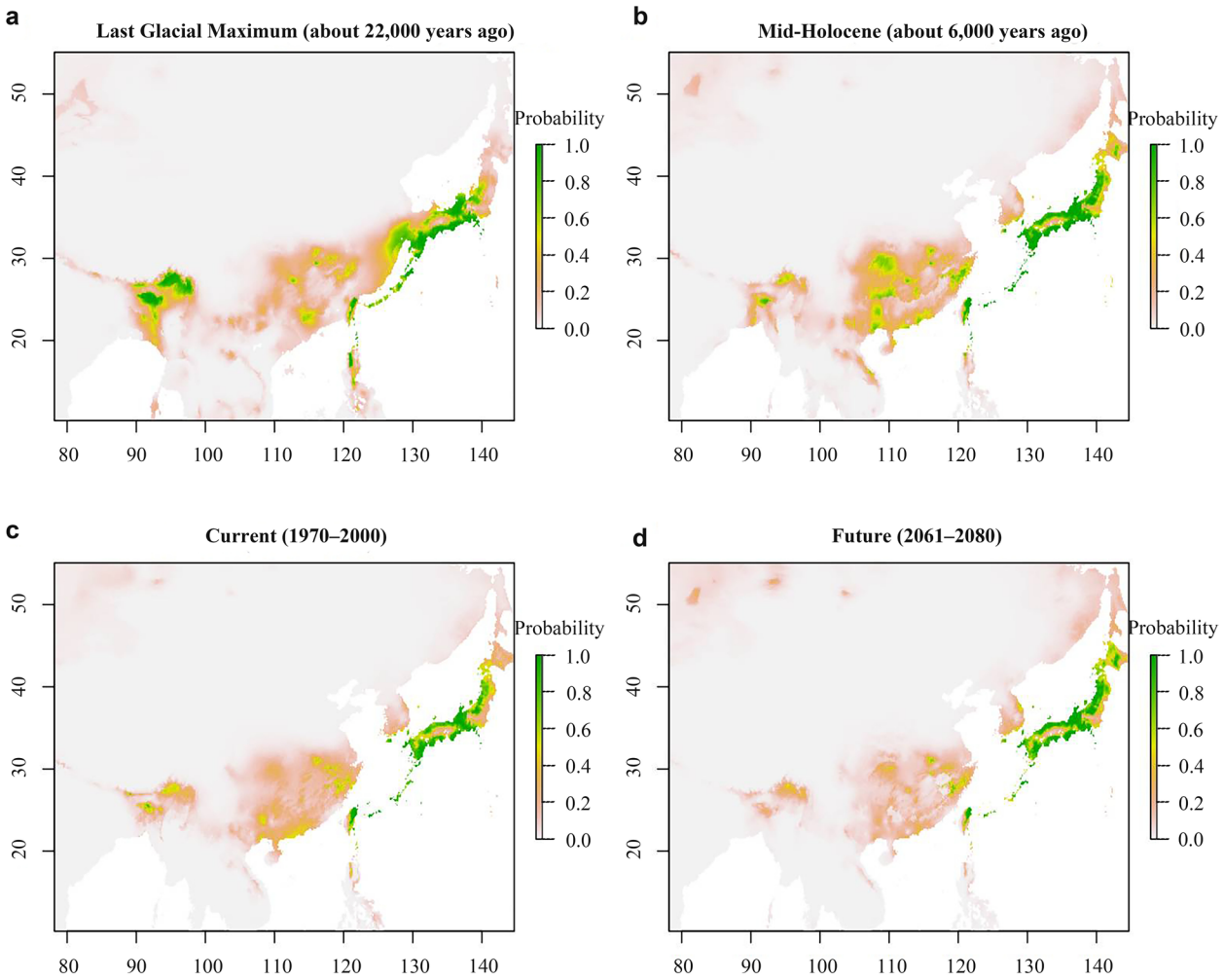

Fig. 4 Species distribution models for *Actinidia rufa*. **a**–**d** The potentially suitable areas for different periods, including Last Glacial Maximum (LGM; **a**); ~22 ka, Mid-Holocene (MH; **b**); 6 ka, current (1970–2000; **c**); and future (2061–2080; **d**). Colors represent the probability of occurrence

To gain further insights into the specific genetic regulation of *A. rufa* in response to waterlogging, WGCNA was conducted using the DEGs identified from *A. rufa* and *A. chinensis* cv. 'Donghong'. This analysis aimed to explore the coexpression networks of the DEGs (Table S3). A total of 45 coexpression modules were identified based on gene expression levels. Importantly, 848 genes preferentially expressed in *A. rufa* after waterlogging treatment were predominantly enriched in the black module (Fig. 6b), while most genes highly expressed in *A. chinensis* cv. 'Donghong' were located in the cyan and brown modules. The heatmap of module-trait correlations indicated that genes in the black module were associated with "oxidative phosphorylation" and metabolites related to fatty acid and amino acid metabolism, including "tryptophan metabolism", "fatty acid degradation and metabolism", and "valine, leucine, and isoleucine degradation" (Fig. 6c).

(See figure on next page.)

Fig. 5 Physiological responses of *Actinidia rufa* and *A. chinensis* 'Donghong' to waterlogging stress**. a** Phenotypes of *A. rufa* and *A. chinensis* 'Donghong' plants after waterlogging treatment for 0, 12, 24, 48, 72 h, and 7 d. **b**–**g** Changes in leaf relative water content (RWC; **b**), hydrogen peroxide (H_2O_2; **c**) content, superoxide dismutase (SOD) activity (**d**), malondialdehyde (MDA) content (**e**), net photosynthetic rate (Pn; **f**), and stomatal conductance (Gs; **g**) in the two cultivars at different time points after treatment. Lowercase letters indicate significant differences in the value between the two cultivars at the same time point ($P < 0.05$)

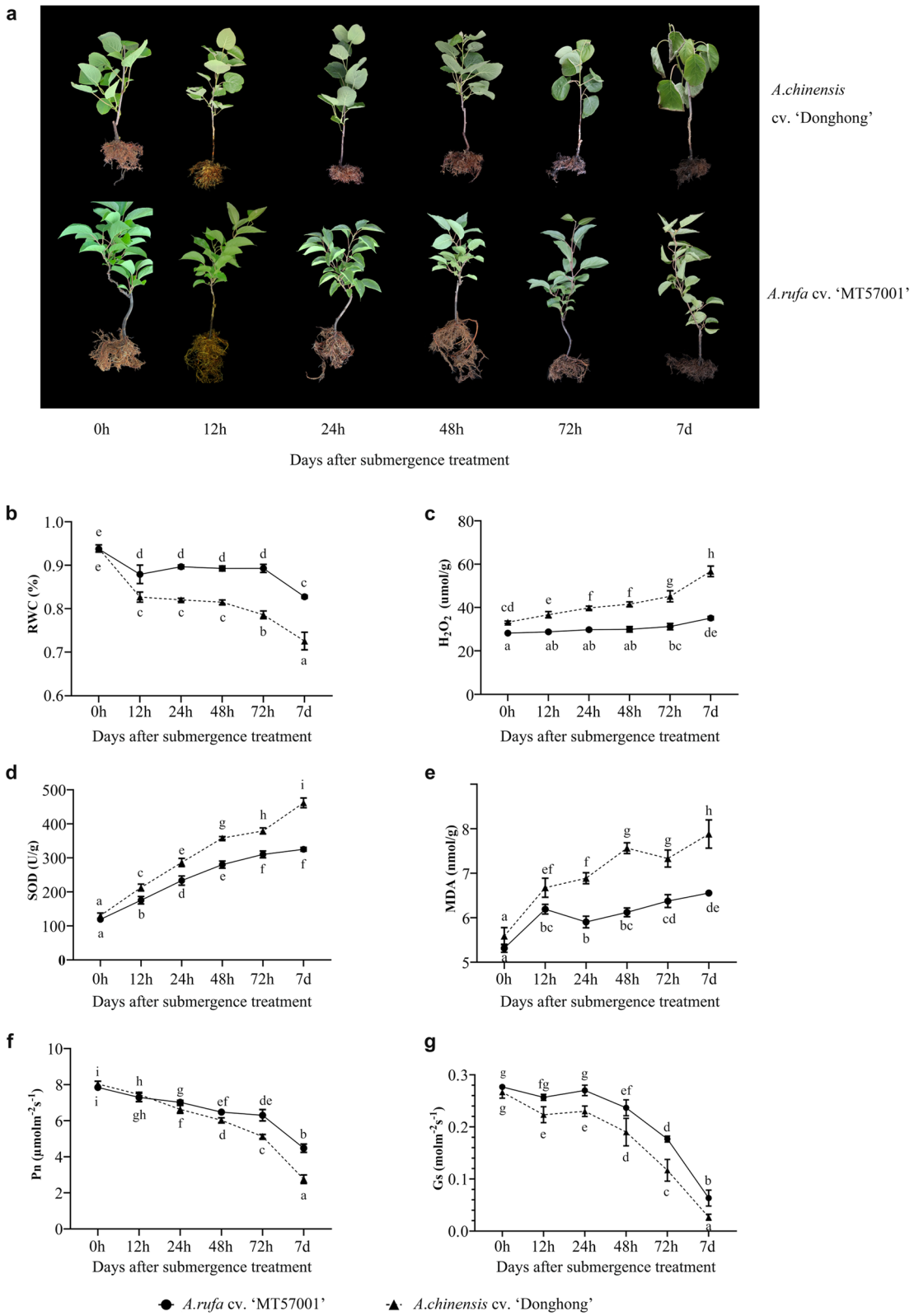

Fig. 5 (See legend on previous page.)

Energy metabolism and endogenous hormones regulate waterlogging tolerance in *A. rufa*

Compared to *A. chinensis* cv. 'Donghong', *A. rufa* exhibited higher expression levels of photosynthesis-related genes (*PsaE* and *PsaL*), suggesting an enhanced ability to adapt to photosynthesis under waterlogging stress (Fig. 6d). The increased expression of these genes during waterlogging likely contributed to mitigating the degree of leaf senescence induced by waterlogging. Notably, *A. rufa* also exhibited positive selection for the gene *HCF136*, which is involved in the assembly of the reaction center (RC) of photosystem II (PHII). Additionally, genes associated with respiratory adaptation were significantly upregulated in *A. rufa*, aiding in overcoming the energy deficit caused by waterlogging stress.

Several genes involved in plant hormone signal transduction, including *xyloglucan endotransglucosylase/hydrolase 22* (*XTH22*), *SAUR36*, *SAUR50*, *EBF2*, *ARR1*, *ARF1*, and *PYL4*, were highly expressed in *A. rufa*, indicating that endogenous plant hormones (Table S4) such as auxin, abscisic acid (ABA), ethylene, and brassinosteroids play critical roles in the species' waterlogging tolerance by inducing stress-related proteins. Importantly, *ABI5-L* and *ERN1*, key regulators of ABA signal transduction and ethylene-responsive factor (ERF) genes, respectively, were positively selected in *A. rufa* compared to other kiwifruit cultivars. The key pathways involved in the biosynthesis and metabolism of these plant hormones are summarized in Fig. 7. Furthermore, root hypoxia-induced inhibition of respiration, leading to energy deficiency, is a primary limiting factor for plants under waterlogging. Notably, this study observed the upregulation of genes related to energy metabolism in *A. rufa* following waterlogging, which could provide the necessary energy supply to withstand waterlogging stress.

Discussion

This study presents a chromosome-level genome assembly and annotation for *A. rufa*, a kiwifruit species notable for its high economic value and exceptional waterlogging tolerance. Although several high-quality kiwifruit genomes have been reported (Huang and Liu 2014; Pilkington et al. 2018; Wu et al. 2019; Tang et al. 2019) and a draft genome of *A. rufa* was recently published (Akagi et al. 2023), a gap-free, high-quality chromosome-level assembly and annotation remained unavailable. This study provides the first comprehensive genome assembly and annotation of *A. rufa*, laying the groundwork for understanding the genetic mechanisms that underpin its waterlogging adaptation. The genome size, GC content, and repetitive element composition of *A. rufa* closely resemble those of other kiwifruit species (Huang et al. 2013; Han et al. 2022; Akagi et al. 2023), indicating a strong degree of genomic conservation across the genus. With this first gap-free genome assembly, further efforts will focus on refining the structural and functional analysis of centromeres (Yue et al. 2023), with an emphasis on resolving centromeric and telomeric regions to enhance structural variant detection and improve annotation accuracy.

Waterlogging stress, caused by soil saturation and oxygen deprivation, severely disrupts root respiration, leading to energy deficits (Pan et al. 2021). Kiwifruit cultivars are generally sensitive to waterlogging, making resistant species such as *A. rufa* valuable for breeding purposes (Chen et al. 2018). Our transcriptomic analysis revealed a rapid upregulation of *XTH22* expression within 12 h of waterlogging treatment. This gene encodes a xyloglucan endotransglucosylase/hydrolase (XET), likely contributing to root adaptation, consistent with previous studies linking XTHs to lateral root development and salt stress responses *via* BES1-dependent pathways (Xu et al. 1996, 2020; Zhang et al. 2022a, b). KEGG enrichment analysis also highlighted the role of WRKY transcription factors in integrating growth and stress signals to optimize plant

(See figure on next page.)

Fig. 6 Transcriptomic dynamics and candidate gene identification under waterlogging stress. **a** Number of differentially expressed genes (DEGs) identified by pairwise comparisons at different time points after waterlogging treatment. Blue bars: upregulated DEGs; green bars: downregulated DEGs. Root tissues of SL and DH plants subjected to waterlogging for 0, 12, 24, 48, and 72 h, designated as R0, R12, R24, R48, and R72, respectively. SL, *Actinidia rufa* cv. 'MTS7001'. **b** Heatmap of DEGs in the black module clustered by weighted gene coexpression network analysis (WGCNA). DH, *A. chinensis* cv. 'Donghong'. **c** Kyoto Encyclopedia of Genes and Genomes (KEGG) pathway enrichment of candidate genes mediating waterlogging tolerance in *A. rufa*. PPAR, peroxisome proliferator-activated receptor. **d** Upregulation of genes involved in energy metabolism and hormone synthesis. *PsaE*, *PsaL*, photosynthesis-related genes; *XTH22*, *xyloglucan endotransglucosylase/hydrolase 22*; *nCBP*, *cellular nucleic-acid binding protein*; *ALDH2B7*, *aldehyde dehydrogenase 2B7*; *MDH*, *Malate dehydrogenase*; *CPPM*, *carboxyvinyl-carboxyphosphonate phosphorylmutase*; *NBD2*, *nucleotide-binding domain 2*; *MPT3*, *mitochondrial phosphate carrier protein 3*; *NDUFS4*, *NADH:ubiquinone oxidoreductase subunit S4*; *ARF1*, *auxin response factor 1*; *AUX22D*, *auxin-induced protein 22D*; *SAUX50/36*, *SAUR-like auxin-responsive protein*; *CYP734a1*, *cytochrome P450 734a1*; *PYL4*, abscisic acid receptor; *EBFs*, *ethylene insensitive 3* (*EIN3*)*-binding F box protein*. **e** Scatter plot of *Ka* and *Ks* calculated with the branch model in CodeML. **f** KEGG enrichment analysis of positively selected genes (PSGs) in *A. rufa*

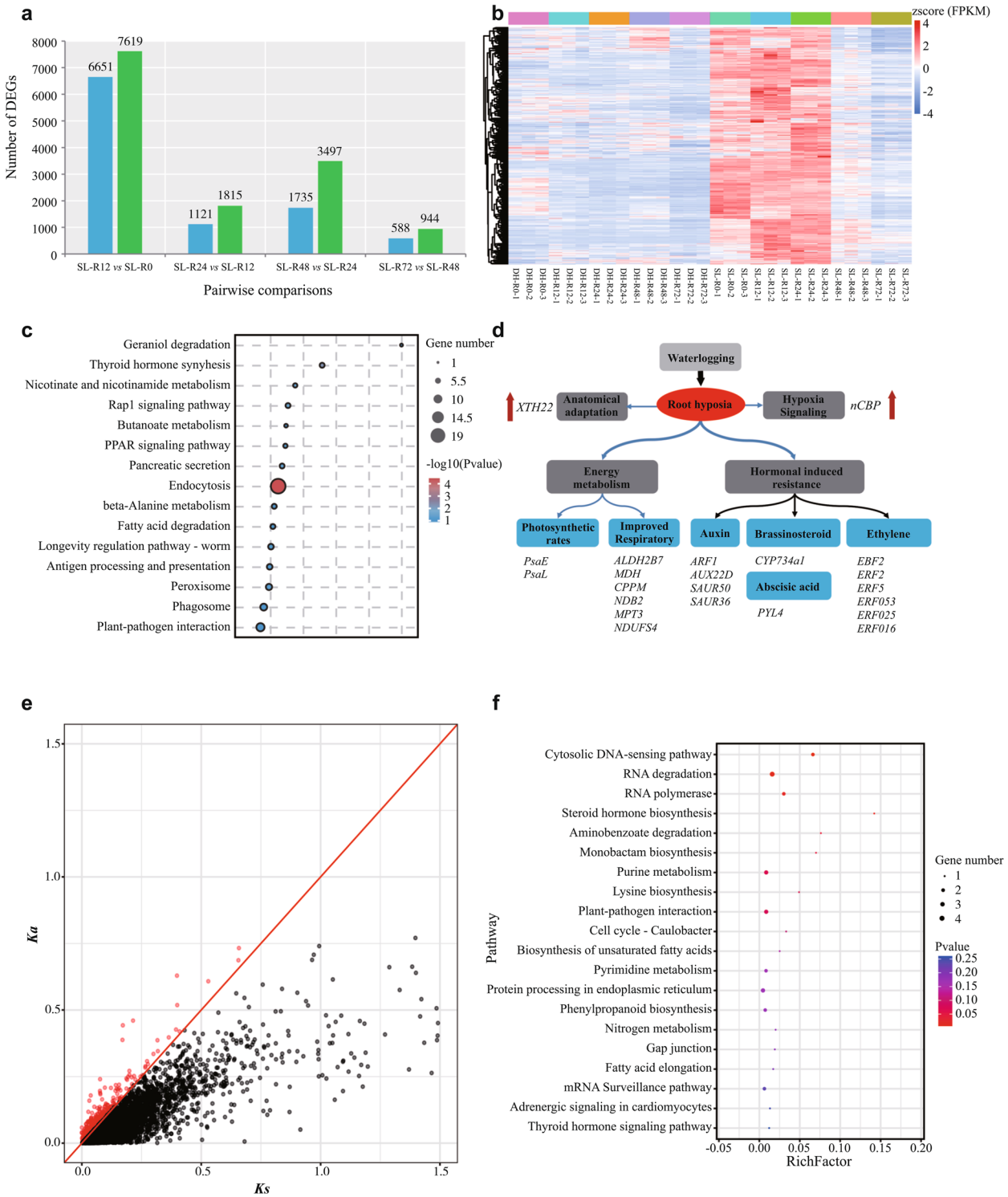

Fig. 6 (See legend on previous page.)

fitness under adverse conditions (Yang et al., 2025). This finding is aligned with studies in citrus (*Citrus junos* cv. Pujiang Xiangcheng), where the expression profile of *PjAP2* was differentially regulated under waterlogging stress (He et al. 2023), further emphasizing the conserved transcriptional mechanisms involved in waterlogging responses across species.

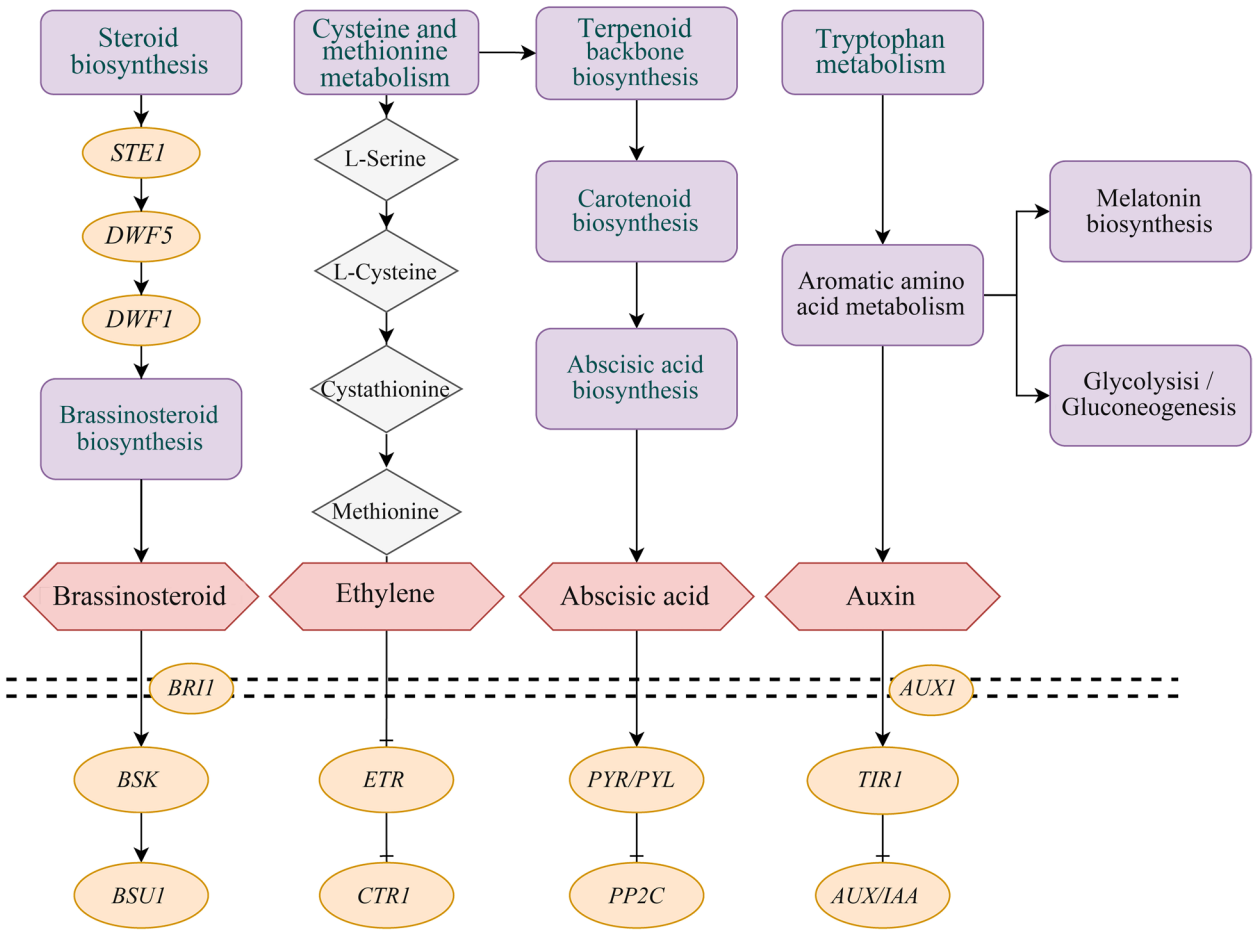

Fig. 7 Hormone-related pathways involved in the regulation of waterlogging stress responses in *Actinidia rufa*. *STE1*, *Salt Tolerance Enhancer 1*; *DWF5*, *Sterol Δ7-sterol-C5-desaturase*; *DWF1*, *Delta-24 Sterol Reductase 1*; *BRI1*, *BAK1-Interacting Receptor-Like Kinase 1*; *BSK*, *Brassinosteroid-Signaling Kinase*; *ETR*, *ethylene response*; *PYR/PYL*, *Pyrabactin Resistance 1/PYR1-Like*; *TIR1*, *Transport Inhibitor Response 1*; *BSU1*, *BRI1-Suppressor 1*; *CTR1*, *Constitutive Triple Response 1*; *PP2C*, *Protein Phosphatase 2C*; *AUX/IAA*, *Auxin/Indole-3-Acetic Acid*

Waterlogging stress typically reduces stomatal conductance, limits CO_2 uptake, and suppresses photosynthesis. Notably, upregulation of photosynthesis-related genes was observed in *A. rufa* under stress, suggesting enhanced photosynthetic plasticity. Waterlogging stress is commonly associated with increased ROS, and improving antioxidant capacity to mitigate oxidative damage has been recognized as a key response to waterlogging (Wang et al. 2024). Preserved photosynthesis plays a critical role in reducing oxidative damage in plants exposed to waterlogging stress (Zheng et al. 2017). Concurrently, genes involved in oxidative phosphorylation and anaerobic fermentation were upregulated in roots, reflecting metabolic adaptations to hypoxia that sustain ATP production (Juntawong et al. 2014; Zhang et al. 2022a, b). These coordinated responses in carbon assimilation and energy metabolism likely represent key components of *A. rufa*'s waterlogging tolerance.

Phytohormonal signaling plays a pivotal role in the adaptation to waterlogging (Pan et al. 2021; Wang et al. 2024). This study observed a significant upregulation of genes involved in the auxin, brassinosteroid, ABA, and ethylene pathways. Ethylene accumulation is an early response to waterlogging that activates auxin transport and promotes adventitious root formation (Alpuerto et al. 2016). ABA has been linked to aerenchyma formation in waterlogged soybean roots (Dong et al. 2024), while brassinosteroids, which interact with auxin, are essential for plant growth and improving abiotic stress tolerance (Zheng et al. 2019). In cucumber, brassinosteroids enhance carbohydrate transfer from leaves to roots under hypoxic conditions, boost glycolytic enzyme activity in roots, and increase antioxidant enzyme activity, reducing ROS production (Nazir et al. 2021). These hormonal signaling pathways likely integrate to coordinate

the morphological and metabolic adaptations observed in *A. rufa*.

Waterlogging tolerance is a complex trait that profoundly impacts kiwifruit production. Enhancing the adaptability of kiwifruit to waterlogging through genetic breeding can substantially increase fruit yields. Most kiwifruit cultivars are particularly sensitive to waterlogging, making *A. rufa* an excellent model for studying the genetic mechanisms behind this trait. AP2/ERF transcription factors, which mediate ethylene signaling, have been shown to be essential for the survival of *A. chinensis* cv. 'Deliciosa' under waterlogging stress (Zhang et al. 2015a, b). Similarly, *A. valvata* has been identified as a waterlogging-resistant rootstock candidate (Gao et al. 2022), with studies demonstrating that its tolerance involves ethylene-mediated aerenchyma formation and root architecture remodeling (Geng et al. 2023). A comparative analysis of *A. rufa* and *A. valvata* may uncover both convergent and distinct mechanisms underlying waterlogging adaptation. The candidate genes identified in this study provide a valuable foundation for future research into the regulatory networks controlling waterlogging responses in kiwifruit. Functional validation of these candidates will be crucial for leveraging their potential in breeding programs.

Conclusions

This study assembled a 613.66 Mb chromosome-scale genome for *A. rufa* (contig N50 = 3.06 Mb; 42,484 PCGs). Phylogenomic analyses confirm that *A. rufa* is a sister lineage to *A. chinensis*, while synteny reconstructions show that a segment of *A. rufa* Chr19 is duplicated onto Chr2 and Chr9 in *A. chinensis*. Compared to *A. chinensis* cv. 'Donghong', *A. rufa* exhibited higher expression levels of genes associated with energy metabolism and hormone-induced resistance, such as those related to auxin, ABA, and brassinosteroids, during the early stages of waterlogging treatment. This study provides valuable insights into the genetic basis of waterlogging tolerance in *A. rufa*, paving the way for future research on molecular breeding strategies for kiwifruits.

Supplementary Information

The online version contains supplementary material available at https://doi.org/10.1007/s44281-026-00103-z.

Supplementary Material 1: Table S1. Genome annotation of repetitive DNA elements in *Actinidia rufa*.

Supplementary Material 2: Table S2. List of 412 genes located within the duplicated regions on Chr19 of the *Actinidia rufa* genome.

Supplementary Material 3: Table S3. Gene clusters generated by weighted gene coexpression network analysis (WGCNA).

Supplementary Material 4: Table S4. Expression levels (FPKM) of genes involved in plant hormone signal transduction.

Supplementary Material 5: Figure S1. 17-mer distribution of Illumina short reads generated by DNA sequencing.

Supplementary Material 6: Figure S2. Demographic history of four kiwifruit (*Actinidia*) species.

Supplementary Material 7: Figure S3. Heatmap of the positively selected genes (PSGs) in *Actinidia rufa*.

Supplementary Material 8: Figure S4. Heatmap of the upregulated positively selected genes (PSGs) in *A. rufa*.

Acknowledgements

We would like to acknowledge the National Kiwifruit Germplasm for providing the kiwifruit germplasm for this experiment.

Authors' contributions

QZ: conceptualization, methodology, investigation, formal analysis, data curation, visualisation, writing—original draft, review and editing. LHW and HZ: methodology, investigation, data curation, writing—review and editing. YLW, ZPW and SKY: data curation, writing—review and editing. YFL and CHZ: supervision, resources, project administration, funding acquisition, writing—review and editing. All authors have read and approved the final manuscript.

Funding

This work was supported by the earmarked fund for the China Agriculture Research System (CARS26), the National Key R&D Program of China (Grant No. 2022YFD1400200), the Scientific and Technological Innovation Project of Hainan Provincial Investment and Holding Group Co., Ltd. (HKKJ2025JBGS09), the Guangxi Science and Technology Major Project (Grant No. Guike AA23023008), and the Hubei Provincial Technological Innovation Program (Grant No. 2024BBB020).

Data availability

The genome sequences and GFF files will be deposited into a public database prior to the acceptance.

Declarations

Ethics approval and consent to participate

Not applicable.

Consent for publication

Not applicable.

Competing interests

The authors declare no financial or non-financial interests.

Received: 8 September 2025 Revised: 14 January 2026 Accepted: 15 January 2026
Published online: 30 April 2026

References

Adey A, Kitzman JO, Burton JN, Daza R, Kumar A, Christiansen L, et al. In vitro, long-range sequence information for de novo genome assembly *via* transposase contiguity. Genome Res. 2014;24:2041–9. https://doi.org/10.1101/gr.178319.114.

Akagi T, Varkonyi-Gasic E, Shirasawa K, Catanach A, Henry IM, Mertten D, et al. Recurrent neo-sex chromosome evolution in kiwifruit. Nat Plants. 2023;9:393–402. https://doi.org/10.1038/s41477-023-01361-9.

Alam I, Lee DG, Kim KH, Park CH, Sharmin SA, Lee H, et al. Proteome analysis of soybean roots under waterlogging stress at an early vegetative stage. J Biosci. 2010;35:49–62. https://doi.org/10.1007/s12038-010-0007-5.

Alpuerto JB, Hussain RMF, Fukao T. The key regulator of submergence tolerance, *SUB1A*, promotes photosynthetic and metabolic recovery from

submergence damage in rice leaves. Plant Cell Environ. 2016;39:672–84. https://doi.org/10.1111/pce.12661.
Bao W, Kojima KK, Kohany O. Repbase update, a database of repetitive elements in eukaryotic genomes. Mob DNA. 2015;6:11. https://doi.org/10.1186/s13100-015-0041-9.
Benson G. Tandem repeats finder: a program to analyze DNA sequences. Nucleic Acids Res. 1999;27:573–80. https://doi.org/10.1093/nar/27.2.573.
Chen S. Ultrafast one-pass FASTQ data preprocessing, quality control, and deduplication using fastp. iMeta. 2023;2:e107. https://doi.org/10.1002/imt2.107.
Chen S, Zhou Y, Chen Y, et al. Fastp: an ultra-fast all-in-one FASTQ preprocessor. Bioinformatics. 2018;34:i884–90. https://doi.org/10.1093/bioinformatics/bty560.
Chin CS, Peluso P, Sedlazeck FJ, Nattestad M, Concepcion GT, Clum A, et al. Phased diploid genome assembly with single-molecule real-time sequencing. Nat Methods. 2016;13:1050–4. https://doi.org/10.1038/nmeth.4035.
De Bie T, Cristianini N, Demuth JP, Hahn MW. CAFE: a computational tool for the study of gene family evolution. Bioinformatics. 2006;22:1269–71. https://doi.org/10.1093/bioinformatics/btl097.
Dong B, Wang Q, Zhou D, Wang Y, Miao Y, Zhong S, et al. Abiotic stress treatment reveals expansin like A gene *OfEXLA1* improving salt and drought tolerance of *Osmanthus fragrans* by responding to abscisic acid. Hortic Plant J. 2024;10:573–85. https://doi.org/10.1016/j.hpj.2022.11.007.
Emms DM, Kelly S. OrthoFinder: phylogenetic orthology inference for comparative genomics. Genome Biol. 2019;20:238. https://doi.org/10.1186/s13059-019-1832-y.
Flynn JM, Hubley R, Goubert C, Rosen J, Clark AG, Feschotte C, et al. RepeatModeler2 for automated genomic discovery of transposable element families. Proc Natl Acad Sci USA. 2020;117:9451–7. https://doi.org/10.1073/pnas.1921046117.
Gao F, Chen C, Arab DA, Du Z, He Y, Ho SYW. EasyCodeML: a visual tool for analysis of selection using CodeML. Ecol Evol. 2019;9:3891–8. https://doi.org/10.1002/ece3.5015.
Gao Y, Jiang Z, Shi M, Zhou Y, Huo L, Li X, et al. Comparative transcriptome provides insight into responding mechanism of waterlogging stress in *Actinidia valvata* Dunn. Gene. 2022;845:146843. https://doi.org/10.1016/j.gene.2022.146843.
Geng S, Lin Z, Xie S, Xiao J, Wang H, Zhao X, et al. Ethylene enhanced waterlogging tolerance by changing root architecture and inducing aerenchyma formation in maize seedlings. J Plant Physiol. 2023;287:154042. https://doi.org/10.1016/j.jplph.2023.154042.
Gubitosa J, Rizzi V, Cignolo D, Fini P, Fanelli F, Cosma P. From agricultural wastes to a resource: kiwi peels, as long-lasting, recyclable adsorbent, to remove emerging pollutants from water. The case of ciprofloxacin removal. Sustain Chem Pharm. 2022;29:100749. https://doi.org/10.1016/j.scp.2022.100749.
Haas BJ, Papanicolaou A, Yassour M, Grabherr M, Blood PD, Bowden J, et al. De novo transcript sequence reconstruction from RNA-seq using the Trinity platform for reference generation and analysis. Nat Protoc. 2013;8:1494–512. https://doi.org/10.1038/nprot.2013.084.
Haas BJ, Salzberg SL, Zhu W, Perțea M, Allen JE, Orvis J, et al. Automated eukaryotic gene structure annotation using EVidenceModeler and the Program to Assemble Spliced Alignments. Genome Biol. 2007;9:R7. https://doi.org/10.1186/gb-2008-9-1-r7.
Han X, Zhang Y, Zhang Q, Ma N, Liu X, Tao W, et al. Two haplotype-resolved, gap-free genome assemblies for *Actinidia latifolia* and *Actinidia chinensis* shed light on the regulatory mechanisms of vitamin C and sucrose metabolism in kiwifruit. Mol Plant. 2022;16:452–70. https://doi.org/10.1016/j.molp.2022.12.022.
He W, Luo L, Xie R, Chai J, Wang H, Wang Y, et al. Genome-wide identification and functional analysis of the AP2/ERF transcription factor family in citrus rootstock under waterlogging stress. Int J Mol Sci. 2023;24:8989. https://doi.org/10.3390/ijms24108989.
Huang H, Liu Y. Natural hybridization, introgression breeding, and cultivar improvement in the genus *Actinidia*. Tree Genet Genomes. 2014;10:1113–22. https://doi.org/10.1007/s11295-014-0771-8.
Huang S, Ding J, Deng D, Tang W, Sun H, Liu D, et al. Draft genome of the kiwifruit *Actinidia chinensis*. Nat Commun. 2013;4:2640. https://doi.org/10.1038/ncomms3640.
Juntawong P, Sirikhachornkit A, Pimjan R, Sonthirod C, Sangsrakru D, Yoocha T, et al. Elucidation of the molecular responses to waterlogging in *Jatropha* roots by transcriptome profiling. Front Plant Sci. 2014;5:658. https://doi.org/10.3389/fpls.2014.00658.
Kim D, Pertea G, Trapnell C, Pimentel H, Kelley R, Salzberg SL. TopHat2: accurate alignment of transcriptomes in the presence of insertions, deletions and gene fusions. Genome Biol. 2013;14:R36. https://doi.org/10.1186/gb-2013-14-4-r36.
Kisaki G, Tanaka S, Ishihara A, Igarashi C, Morimoto T, Hamano K, et al. Evaluation of various cultivars of *Actinidia* species and breeding source *Actinidia rufa* for resistance to *Pseudomonas syringae* pv. *actinidiae* biovar 3. J Gen Plant Pathol. 2018;84:399–406. https://doi.org/10.1007/s10327-018-0804-5.
Kumar R, Bohra A, Pandey AK, Pandey MK, Kumar A. Metabolomics for plant improvement: status and prospects. Front Plant Sci. 2017;8:1302. https://doi.org/10.3389/fpls.2017.01302.
Langfelder P, Horvath S. WGCNA: an R package for weighted correlation network analysis. BMC Bioinformatics. 2008;9:559. https://doi.org/10.1186/1471-2105-9-559.
Li B, Li X, Wang Y, Liu X, Li K, Li R, et al. KPGD: a kiwifruit pangenome database for comprehensive mining of genetic diversity in the genus *Actinidia*. Plant Commun. 2025;6:101373. https://doi.org/10.1016/j.xplc.2025.101373.
Li H, Durbin R. Fast and accurate short read alignment with Burrows-Wheeler transform. Bioinformatics. 2009;25:1754–60. https://doi.org/10.1093/bioinformatics/btp324.
Liu Y, Li D, Zhang Q, Song C, Zhong C, Zhang X, et al. Rapid radiations of both kiwifruit hybrid lineages and their parents shed light on a two-layer mode of species diversification. New Phytol. 2017;215:877–90. https://doi.org/10.1111/nph.14607.
Love MI, Huber W, Anders S. Moderated estimation of fold change and dispersion for RNA-seq data with DESeq2. Genome Biol. 2014;15:550. https://doi.org/10.1186/s13059-014-0550-8.
McKenna A, Hanna M, Banks E, Sivachenko A, Cibulskis K, Kernytsky A, et al. The Genome Analysis Toolkit: a MapReduce framework for analyzing next-generation DNA sequencing data. Genome Res. 2010;20:1297–303. https://doi.org/10.1101/gr.107524.110.
Miller SA, Smith GS, Cookson JH. The effects of transient waterlogging on different species of *Actinidia*. Acta Hortic. 1997;444:323–8. https://doi.org/10.17660/ActaHortic.1997.444.50.
Nachtweide S, Stanke M. Multi-genome annotation with AUGUSTUS. Methods Mol Biol. 2019;1962:139–60. https://doi.org/10.1007/978-1-4939-9173-0_8.
Nazir F, Fariduddin Q, Hussain A, Khan TA. Brassinosteroid and hydrogen peroxide improve photosynthetic machinery, stomatal movement, root morphology and cell viability and reduce Cu-triggered oxidative burst in tomato. Ecotoxicol Environ Saf. 2021;207:111081. https://doi.org/10.1016/j.ecoenv.2020.111081.
Pan J, Sharif R, Xu X, Chen X. Mechanisms of waterlogging tolerance in plants: research progress and prospects. Front Plant Sci. 2021;11:627331. https://doi.org/10.3389/fpls.2020.627331.
Pilkington SM, Crowhurst R, Hilario E, Nardozza S, Fraser L, Peng Y, et al. A manually annotated *Actinidia chinensis* var. *chinensis* (kiwifruit) genome highlights the challenges associated with draft genomes and gene prediction in plants. BMC Genomics. 2018;19:257. https://doi.org/10.1186/s12864-018-4656-3.
Price MN, Dehal PS, Arkin AP. FastTree: computing large minimum evolution trees with profiles instead of a distance matrix. Mol Biol Evol. 2009;26:1641–50. https://doi.org/10.1093/molbev/msp077.
Sanz V, López-Hortas L, Torres MD, Domínguez H. Trends in kiwifruit and byproducts valorization. Trends Food Sci Technol. 2021;107:401–14. https://doi.org/10.1016/j.tifs.2020.11.010.
Simao FA, Waterhouse RM, Ioannidis P, Kriventseva EV, Zdobnov EM. BUSCO: assessing genome assembly and annotation completeness with single-copy orthologs. Bioinformatics. 2015;31:3210–2. https://doi.org/10.1093/bioinformatics/btv351.
Slater GSC, Birney E. Automated generation of heuristics for biological sequence comparison. BMC Bioinformatics. 2005;6:31. https://doi.org/10.1186/1471-2105-6-31.
Suezawa K, Fukuda T, Mizutani R, Yamashita T, Otani M, Abe M, et al. Field performance of tetraploid *Actinidia chinensis* 'Sanuki Gold' on *Actinidia*

rufa rootstocks. Acta Hortic. 2018;1218:413–8. https://doi.org/10.17660/ActaHortic.2018.1218.57.
Suleria HAR, Barrow CJ, Dunshea FR. Screening and characterization of phenolic compounds and their antioxidant capacity in different fruit peels. Foods. 2020;9:1206. https://doi.org/10.3390/foods9091206.
Tang H, Krishnakumar V, Zeng X, Xu Z, Taranto A, Lomas JS, et al. JCVI: a versatile toolkit for comparative genomics analysis. Imeta. 2024;3:e211. https://doi.org/10.1002/imt2.211.
Tang W, Sun X, Yue J, Tang X, Jiao C, Yang Y, et al. Chromosome-scale genome assembly of kiwifruit *Actinidia eriantha* with single-molecule sequencing and chromatin interaction mapping. Gigascience. 2019;8:giz027. https://doi.org/10.1093/gigascience/giz027.
Tarailo-Graovac M, Chen N. Using RepeatMasker to identify repetitive elements in genomic sequences. Curr Protoc Bioinformatics. 2009;25:4.10.1-4.10.14. https://doi.org/10.1002/0471250953.bi0410s25.
Terhorst J, Kamm JA, Song YS. Robust and scalable inference of population history from hundreds of unphased whole genomes. Nat Genet. 2017;49:303–9. https://doi.org/10.1038/ng.3748.
Vollering J, Halvorsen R, Mazzoni S. The MIAmaxent R package: variable transformation and model selection for species distribution models. Ecol Evol. 2019;9:12051–68. https://doi.org/10.1002/ece3.5654.
Wang S, Qiu Y, Zhu F. Kiwifruit (*Actinidia* spp.): a review of chemical diversity and biological activities. Food Chem. 2021;350:128469. https://doi.org/10.1016/j.foodchem.2020.128469.
Wang X, Cao M, Li H, Liu Y, Fan S, Zhang N, et al. Strategies and prospects for melatonin to alleviate abiotic stress in horticultural plants. Hortic Plant J. 2024;10:601–14. https://doi.org/10.1016/j.hpj.2023.03.011.
Wang Y, Dong J, Yuan X, Zheng H, Zhong C, Zhang Q. Cracking the kiwifruit code: how cultivar and origin co-create premium quality and consumer appeal. Future Foods. 2025;11:100651. https://doi.org/10.1016/j.fufo.2025.100651.
Wang Y, Dong M, Wu Y, Zhang F, Ren W, Lin Y, et al. Telomere-to-telomere and haplotype-resolved genome of the kiwifruit *Actinidia eriantha*. Mol Hortic. 2023;3:4. https://doi.org/10.1186/s43897-023-00052-5.
Wu H, Ma T, Kang M, Ai F, Zhang J, Dong G, et al. A high-quality *Actinidia chinensis* (kiwifruit) genome. Hortic Res. 2019;6:117. https://doi.org/10.1038/s41438-019-0202-y.
Wu H, Yang W, Dong G, Hu Q, Li D, Liu J. Construction of the super pan-genome for the genus *Actinidia* reveals structural variations linked to phenotypic diversity. Hortic Res. 2025a;12:uhaf067. https://doi.org/10.1093/hr/uhaf067.
Wu L, Dong J, Zheng H, Wang Y, Han F, Yang S, et al. Transcription factor AcNAC056 and AcMADS1 regulate gibberellin 2-oxidase gene *AcGA2ox1* induced parthenocarpy in *Actinidia eriantha*. Int J Biol Macromol. 2025b;322:146917. https://doi.org/10.1016/j.ijbiomac.2025.146917.
Wu L, Dong J, Zheng H, Wang Y, Qiu D, Atak A, et al. Effects of plant growth regulator (2,4-D) treatments on fruit development and chemical content in the kiwifruit plant (*Actinidia chinensis*). BMC Plant Biol. 2025c;25:1073. https://doi.org/10.1186/s12870-025-07138-w.
Xia H, Deng H, Li M, Xie Y, Lin L, Zhang H, et al. Chromosome-scale genome assembly of a natural diploid kiwifruit (*Actinidia chinensis* var. *deliciosa*). Sci Data. 2023;10:92. https://doi.org/10.1038/s41597-023-02006-4.
Xu L, Miao T, Cui Z, Varkonyi-Gasic E, Zhang A, Wang L, et al. Synteny-based comparative pan-genome reveals a male-specific FT gene underlying flowering time dimorphism in kiwifruit. Plant J. 2026;125:e70664. https://doi.org/10.1111/tpj.70664.
Xu P, Fang S, Chen H, Cai W. The brassinosteroid-responsive xyloglucan endotransglucosylase/hydrolase 19 (*XTH19*) and *XTH23* genes are involved in lateral root development under salt stress in Arabidopsis. Plant J. 2020;104:59–75. https://doi.org/10.1111/tpj.14905.
Xu W, Campbell P, Vargheese AK, Braam J. The Arabidopsis XET-related gene family: environmental and hormonal regulation of expression. Plant J. 1996;9:879–89. https://doi.org/10.1046/j.1365-313x.1996.9060879.x.
Xu Z, Wang H. LTR_FINDER: an efficient tool for the prediction of full-length LTR retrotransposons. Nucleic Acids Res. 2007;35:W265–8. https://doi.org/10.1093/nar/gkm286.
Yang L, Fang S, Liu L, Zhao L, Chen W, Li X, et al. WRKY transcription factors: hubs for regulating plant growth and stress responses. J Integr Plant Biol. 2025;67:488–509. https://doi.org/10.1111/jipb.13828.
Yang Z. PAML 4: phylogenetic analysis by maximum likelihood. PAML4: Phylogenetic Analysis by Maximum Likelihood Mol Biol Evol. 2007;24:1586–91. https://doi.org/10.1093/molbev/msm088.
Yao X, Wang S, Wang Z, Li D, Jiang Q, Zhang Q, et al. The genome sequencing and comparative analysis of a wild kiwifruit *Actinidia eriantha*. Mol Hortic. 2022;2:13. https://doi.org/10.1186/s43897-022-00034-z.
Yu X, Qin M, Qu M, Jiang Q, Guo S, Chen Z, et al. Genomic analyses reveal dead-end hybridization between two deeply divergent kiwifruit species rather than homoploid hybrid speciation. Plant J. 2023;115:1528–43. https://doi.org/10.1111/tpj.16336.
Yuan X, Zheng H, Fan J, Liu F, Li J, Zhong C, et al. Comparative study on physicochemical and nutritional qualities of kiwifruit varieties. Foods. 2022;12:108. https://doi.org/10.3390/foods12010108.
Yue J, Chen Q, Wang Y, Zhang L, Ye C, Wang X, et al. Telomere-to-telomere and gap-free reference genome assembly of the kiwifruit *Actinidia chinensis*. Hortic Res. 2023;10:uhac264. https://doi.org/10.1093/hr/uhac264.
Zhang C, He M, Jiang Z, Liu L, Pu J, Zhang W, et al. The xyloglucan endotransglucosylase/hydrolase gene *XTH22/TCH4* regulates plant growth by disrupting the cell wall homeostasis in *Arabidopsis* under boron deficiency. Int J Mol Sci. 2022a;23:1250. https://doi.org/10.3390/ijms23031250.
Zhang H, Li G, Yan C, Zhang X, Cao N, Le M, et al. Elucidating the molecular responses to waterlogging stress in *Cucumis melo* by comparative transcriptome profiling. Horticulturae. 2022b;8:891. https://doi.org/10.3390/horticulturae8100891.
Zhang J, Huang S, Mo Z, Xuan J, Jia X, Wang G, et al. De novo transcriptome sequencing and comparative analysis of differentially expressed genes in kiwifruit under waterlogging stress. Mol Breed. 2015a;35:1–12. https://doi.org/10.1007/s11032-015-0408-0.
Zhang L, Tang Z, Zheng H, Zhong C, Zhang Q. Comprehensive analysis of metabolome and transcriptome in fruits and roots of kiwifruit. Int J Mol Sci. 2023;24:1299. https://doi.org/10.3390/ijms24021299.
Zhang Q, Liu C, Liu Y, VanBuren R, Yao X, Zhong C, et al. High-density interspecific genetic maps of kiwifruit and the identification of sex-specific markers. DNA Res. 2015b;22:367–75. https://doi.org/10.1093/dnares/dsv019.
Zhang Z, Xiao J, Wu J, Zhang H, Liu G, Wang X, et al. ParaAT: a parallel tool for constructing multiple protein-coding DNA alignments. Biochem Biophys Res Commun. 2012;419:779–81. https://doi.org/10.1016/j.bbrc.2012.02.101.
Zheng L, Gao C, Zhao C, Zhang L, Han M, An N, et al. Effects of brassinosteroid associated with auxin and gibberellin on apple tree growth and gene expression patterns. Hortic Plant J. 2019;5:93–108. https://doi.org/10.1016/j.hpj.2019.04.006.
Zheng X, Zhou J, Tan DX, Wang N, Wang L, Shan D, et al. Melatonin improves waterlogging tolerance of *Malus baccata* (Linn.) Borkh. seedlings by maintaining aerobic respiration, photosynthesis and ROS migration. Front Plant Sci. 2017;8:483. https://doi.org/10.3389/fpls.2017.00483.
Zhong C, Li D, Zhang Q, Li L, Huang W, Han, F. Identification, creation and utilization of the germplasm resources of kiwifruit. Acta Hortic. 2024;1401:17–24. https://doi.org/10.17660/ActaHortic.2024.1401.3.
Zhou Y, Zhang Z, Zhao X, Liu L, Tang Q, Fu J, et al. Receptor-like cytoplasmic kinase STK confers salt tolerance in rice. Rice. 2023;16:21. https://doi.org/10.1186/s12284-023-00637-0.
Zimin AV, Salzberg SL. The genome polishing tool POLCA makes fast and accurate corrections in genome assemblies. PLoS Comput Biol. 2020;16:e1007981. https://doi.org/10.1371/journal.pcbi.1007981.

Publisher's Note